

Supplementary Information for

Lanthanum doping enabling high drain current modulation in a p-type tin monoxide thin-film transistor

Sungyeon Yim¹, Taikyu Kim¹, Baekyun Yu¹, Xu Hongwei¹, Yong Youn², Seungwu Han², and Jae Kyeong Jeong¹

¹Department of Electronic Engineering, Hanyang University, Seoul 04763, South Korea

²Department of Materials Science and Engineering, Seoul National University, Seoul 08826, Korea

AUTHOR EMAIL ADDRESS: J. K. Jeong (jkjeong1@hanyang.ac.kr)

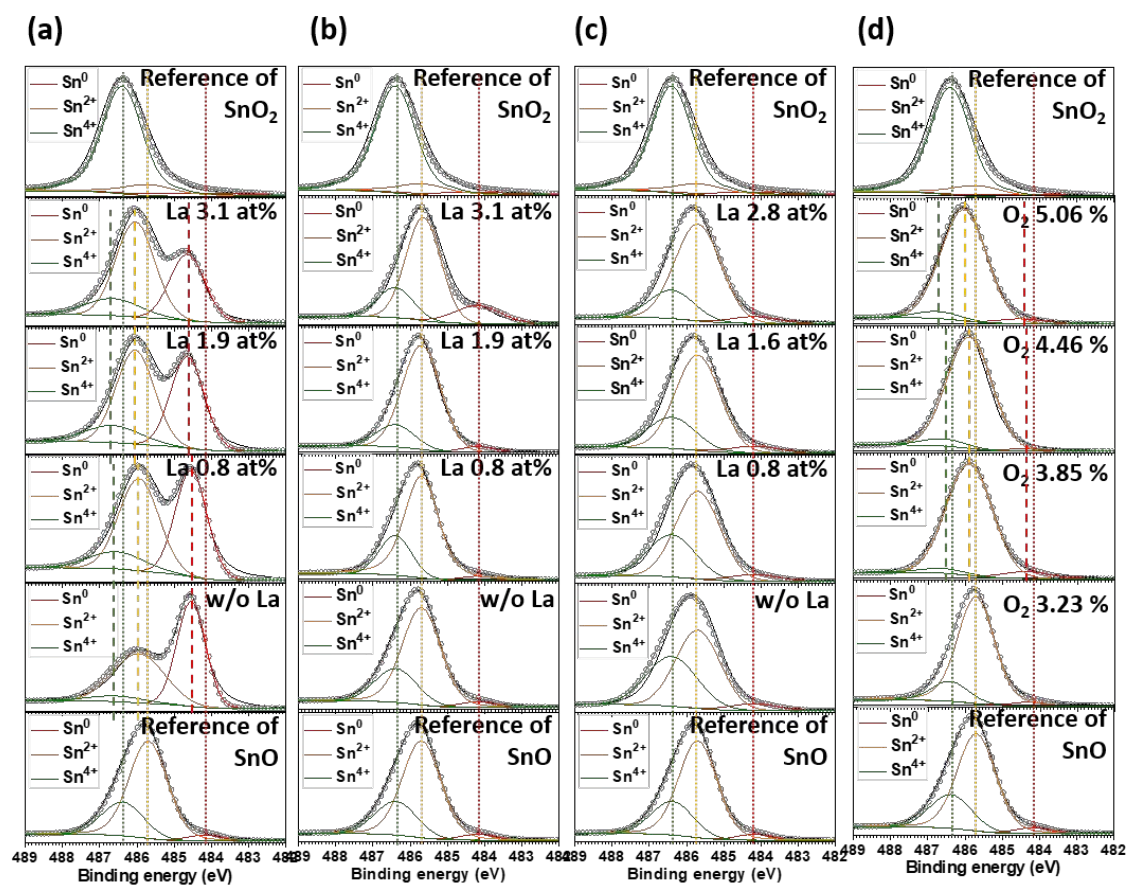


Figure S1. XP spectra of Sn $3d_{5/2}$ for the SnO films with different La loadings (a) before PDA, (b) after PDA at 250 °C, and (c) after PDA at 300 °C. (d) XP spectra of Sn $3d_{5/2}$ for the SnO films with different oxygen pressure on 1.9 at% loadings after PDA at 250 °C.

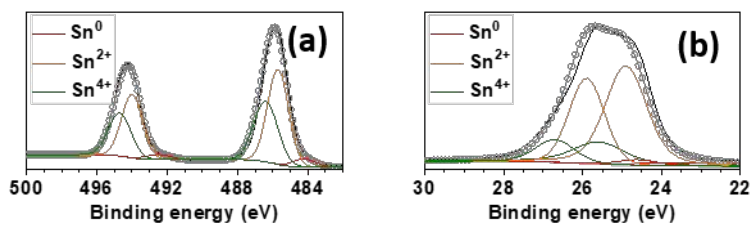


Figure S2. XP spectra of (a) Sn 3d and (b) Sn 4d for the La-free SnO films post-annealed at 250 °C for 1 hr.

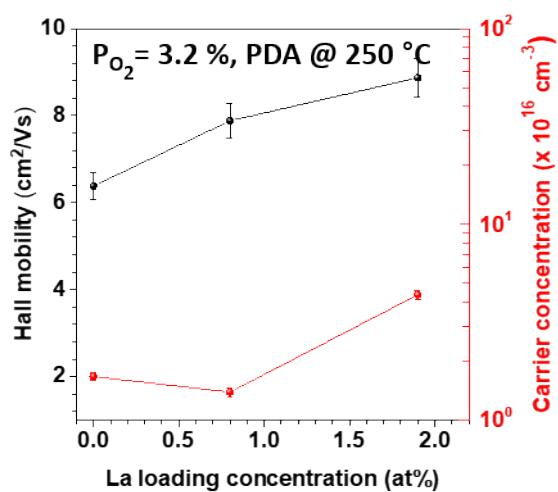


Figure S3. Electrical properties of 250 °C annealed SnO films with different La loadings from Hall effect measurement. Black line (left y-axis) is Hall mobility, and red line (right y-axis) is a free hole carrier concentration measured from Hall measurement.

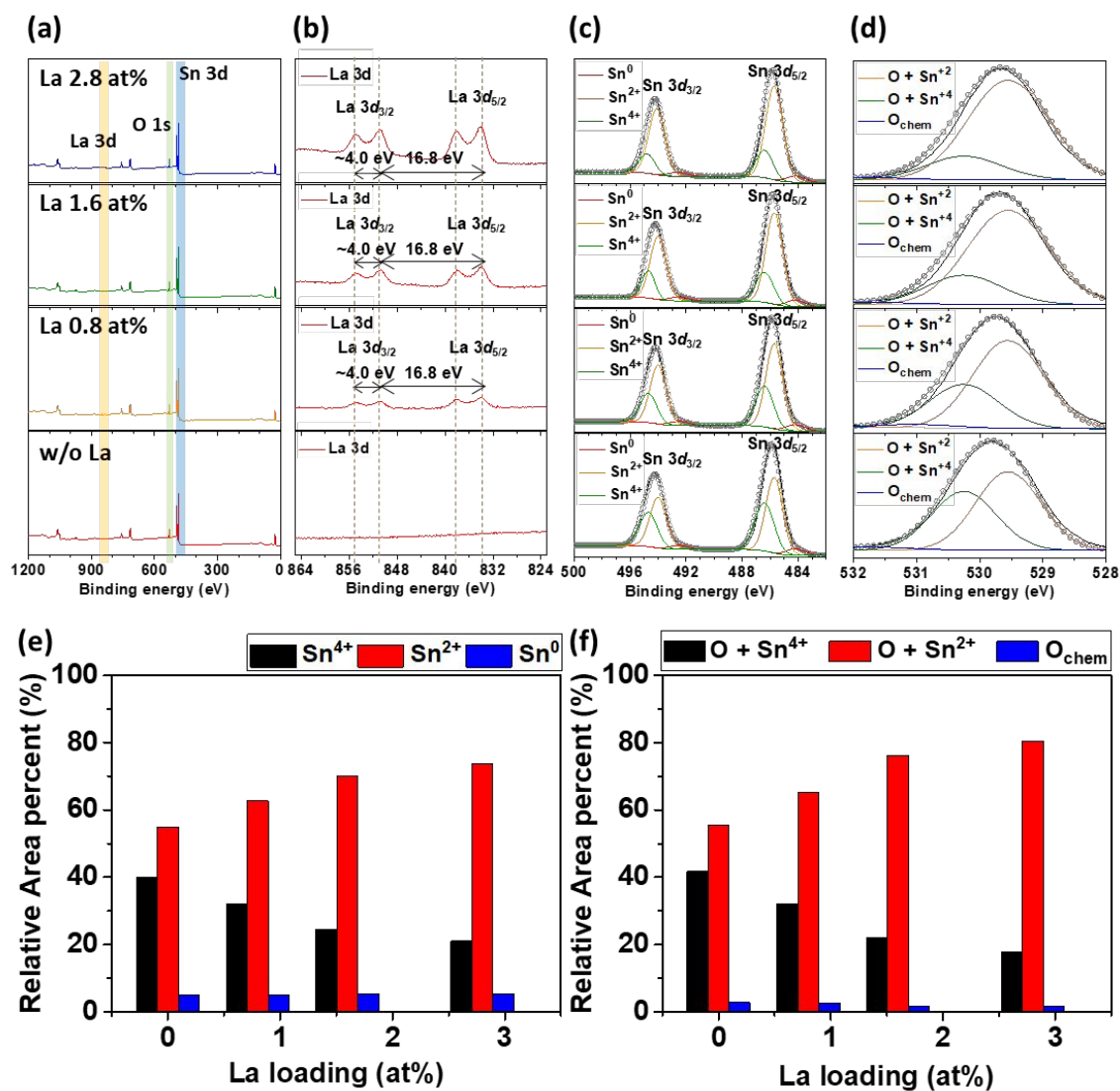


Figure S4. (a) XPS survey spectra, XP spectra of (b) La 3d, (c) Sn 3d, and (d) O 1s for the SnO films annealed in 300 °C with different La loadings. Chemical compositions including Sn⁰, Sn²⁺, and Sn⁴⁺ of SnO films with different La loadings, which were de-convoluted from XP spectra of (e) Sn 3d and (f) O 1s.

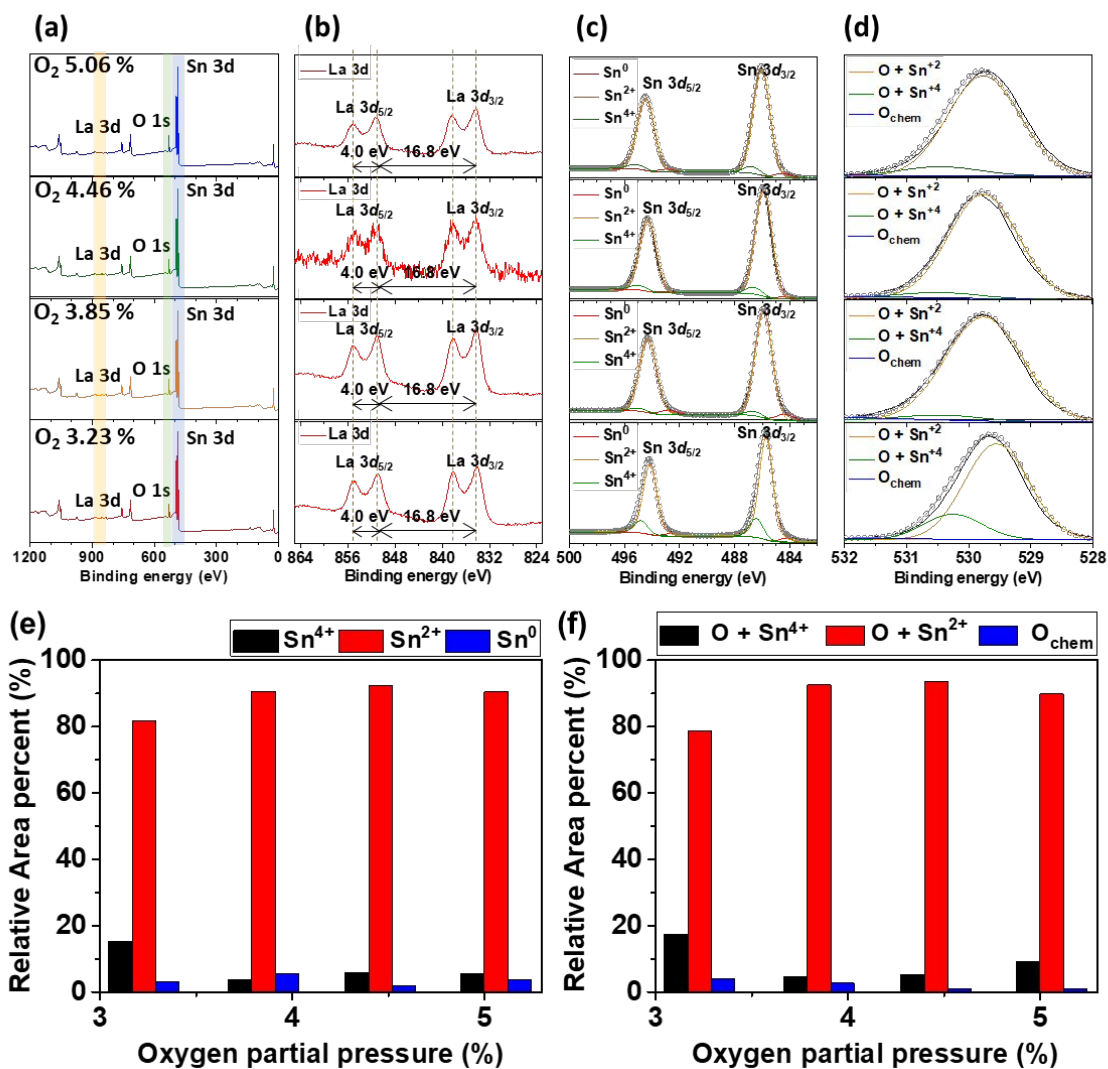


Figure S5. (a) XPS survey spectra, XP spectra of (b) La 3d, (c) Sn 3d, and (d) O 1s for the SnO films annealed at 250 °C with different oxygen pressure on 1.9 at% loadings. Chemical compositions including Sn⁰, Sn²⁺, and Sn⁴⁺ of SnO films with different oxygen pressure on 1.9 at% La loadings, which were de-convoluted from XP spectra of (e) Sn 3d and (f) O 1s.

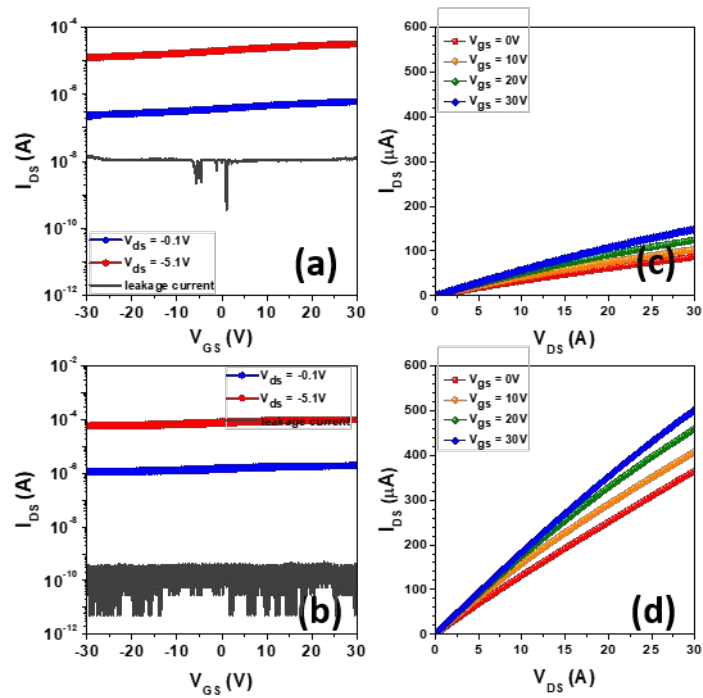


Figure S6. Transfer characteristics of the SnO TFTs with different La loadings of (a) 0 at% and (b) 1.9 at% after the PDA at 250 °C for 1 hr under the forming gas atmosphere. The corresponding output characteristics of the SnO TFTs with different La loadings of (c) 0 at% and (d) 1.9 at%.

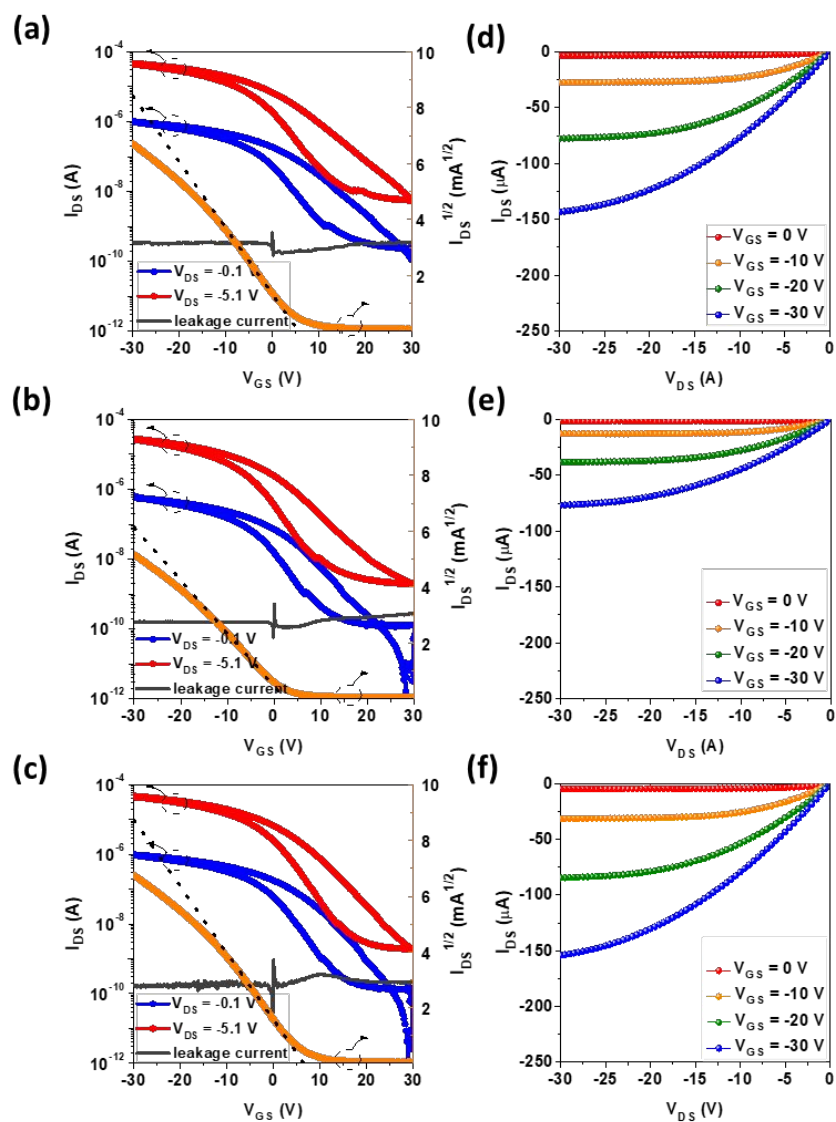


Figure S7. Transfer characteristics of the 1.9 at% La-loaded SnO TFTs annealed in 250 °C with different oxygen partial pressures of (a) 3.23 %, (b) 3.85 at%, and (c) 4.46 at%. The corresponding output characteristics of the 1.9 at% La-loaded SnO TFTs with oxygen partial pressures of (d) 3.23 %, (e) 3.85 %, and (f) 4.46 %.

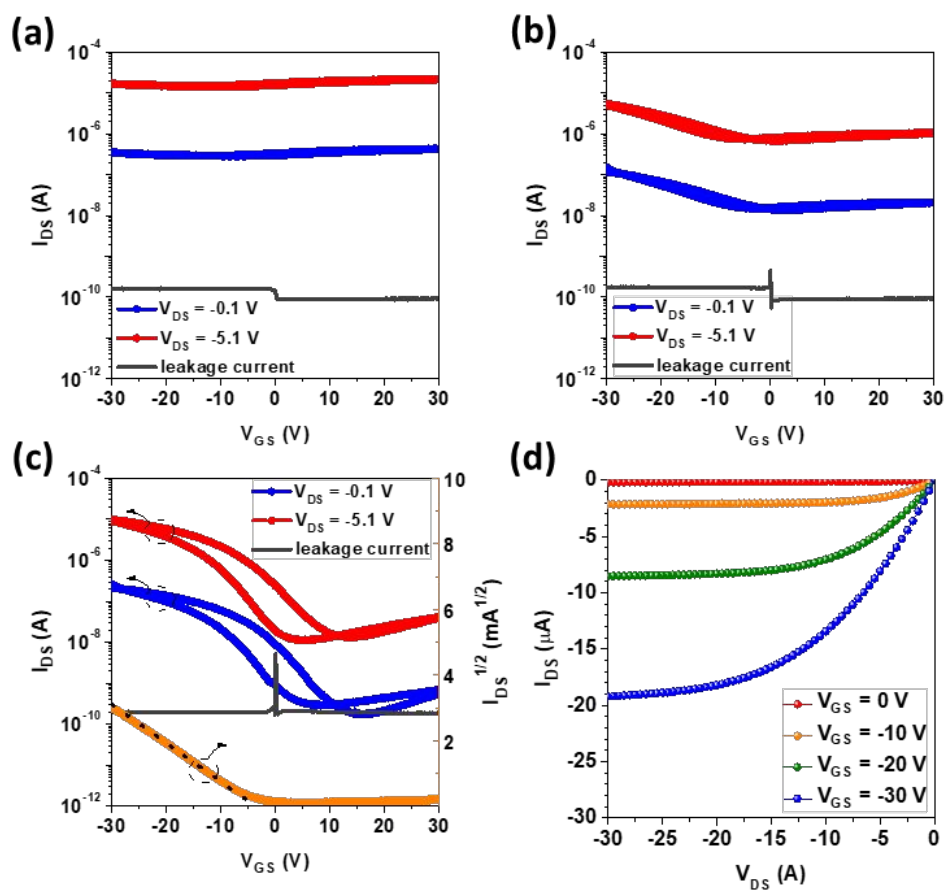


Figure S8. Transfer characteristics of the SnO TFTs annealed at 300 °C with different La loadings of (a) 0 at%, (b) 0.8 at%, and (c) 1.9 at%. (d) The output characteristics of the SnO TFTs with 1.9 at% La loadings

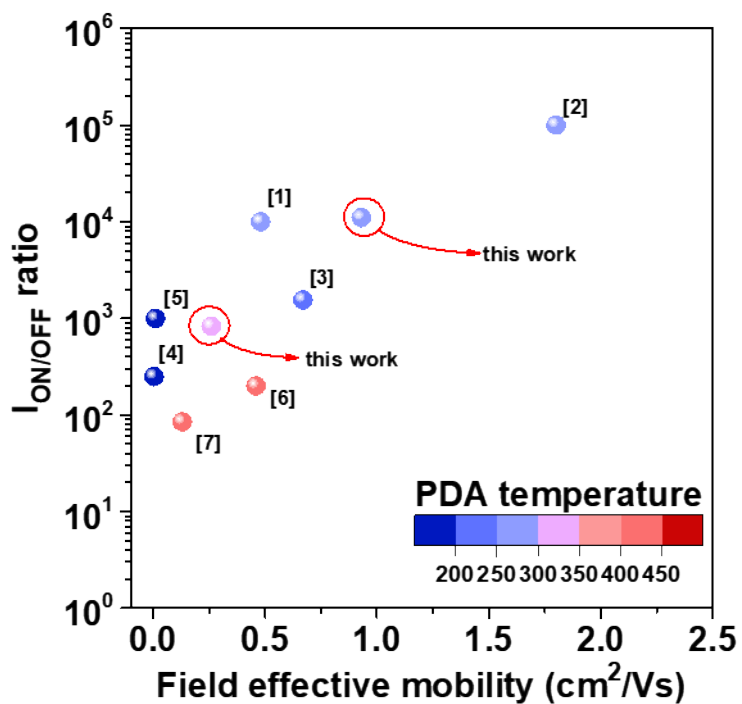


Figure S9. Comparisons of the trade-off between the saturation mobility and $I_{ON/OFF}$ ratio for the SnO TFTs fabricated at the various annealing temperatures. For fair comparison, the SnO TFTs with SiO_2 gate dielectric and non-passivated devices were collected. It can be shown that the performances of SnO TFTs reported in the literatures were deteriorated at the higher annealing temperature (> 300 $^{\circ}\text{C}$) compared to those at the lower annealing temperature (< 300 $^{\circ}\text{C}$). The introduction of La cation into the SnO channel allowed the resulting transistor to exhibit the higher mobility and $I_{ON/OFF}$ ratio due to the La-induced efficient suppression of Sn^{4+} , as shown in Figure 8b.

Table S1. Chemical compositions including Sn⁰, Sn²⁺, and Sn⁴⁺ of the La-free SnO films post-annealed at 250 °C for 1 hr states, which was de-convoluted from XP spectra of Sn 3d_{5/2} and Sn 4d_{5/2}.

| XP Spectra | Sn ⁰ (%) | Sn ²⁺ (%) | Sn ⁴⁺ (%) |
|----------------------|---------------------|----------------------|----------------------|
| Sn 3d _{5/2} | 3.8 | 70.9 | 25.3 |
| Sn 4d _{5/2} | 5.7 | 69.7 | 24.6 |

Table S2. Chemical compositions including Sn⁰, Sn²⁺, and Sn⁴⁺ of as deposited SnO films with different La loadings, which were de-convoluted from XP spectra of Sn 3d and O 1s.

| La Loading in SnO film [at%] | Sn 3d | | | O 1s | | |
|------------------------------|---|---|--|-------------------------------------|--------------------------------------|--------------------------------------|
| | Sn ⁴⁺ (486.8 ± 0.1 eV) | Sn ²⁺ (486.1 ± 0.1 eV) | Sn ⁰ (484.6 ± 0.1 eV) | O _{chem} (531.75 eV) | O+Sn ⁴⁺ (530.25 eV) | O+Sn ²⁺ (529.55 eV) |
| 0 | 5.4 | 43.2 | 51.4 | 4.1 | 41.7 | 54.2 |
| 0.8 | 11.7 | 46.1 | 42.2 | 4.5 | 38.8 | 56.7 |
| 1.9 | 12.5 | 47.2 | 40.3 | 0.8 | 41.1 | 58.1 |
| 3.1 | 13.7 | 53.0 | 33.3 | 4.4 | 34.0 | 61.6 |

Table S3. Chemical compositions including Sn⁰, Sn²⁺, and Sn⁴⁺ of SnO films annealed at 250 °C with different La loadings, which were de-convoluted from XP spectra of Sn 3d and O 1s.

| La Loading in SnO film [at%] | Sn 3d | | | O 1s | | |
|------------------------------|---|---|--|-------------------------------------|--------------------------------------|--------------------------------------|
| | Sn ⁴⁺ (486.4 ± 0.3 eV) | Sn ²⁺ (485.7 ± 0.3 eV) | Sn ⁰ (484.2 ± 0.3 eV) | O _{chem} (531.75 eV) | O+Sn ⁴⁺ (530.25 eV) | O+Sn ²⁺ (529.55 eV) |
| 0 | 25.3 | 70.9 | 3.8 | 3.7 | 27.4 | 68.9 |
| 0.8 | 23.4 | 74.2 | 2.4 | 3.8 | 23.1 | 73.1 |
| 1.9 | 16.9 | 79.7 | 3.4 | 3.9 | 17.4 | 78.7 |
| 3.1 | 19.2 | 65.4 | 15.4 | 3.1 | 33.7 | 63.2 |

Table S4. Hall effect measurements for the SnO films with different La loadings of 0 and 1.9 at%, which were annealed in forming gas atmosphere in 250 °C.

| La Loading in SnO film [at%] | majority carrier type | μ_{Hall} (cm^2/Vs) | N_{Hall} (cm^{-3}) |
|---------------------------------|--------------------------|--|---|
| 0 | electron | 1.2 ± 0.9 | $4.0 (\pm 2.7) \times 10^{18}$ |
| 1.9 | electron | 3.5 ± 3.7 | $1.7 (\pm 0.9) \times 10^{19}$ |

Table S5. Chemical compositions including Sn⁰, Sn²⁺, and Sn⁴⁺ of SnO films annealed at 250 °C with different oxygen pressure on 1.9 at% La loadings, which were de-convoluted from XP spectra of Sn 3d and O 1s.

| Oxygen partial pressure [%] | Sn 3d | | | O 1s | | |
|--------------------------------------|---|---|--|---|--|--|
| | Sn ⁴⁺ (486.4 ± 0.3 eV) | Sn ²⁺ (485.7 ± 0.3 eV) | Sn ⁰ (484.2 ± 0.3 eV) | O _{chem} (531.75 ± 0.2 eV) | O+Sn ⁴⁺ (530.25 ± 0.2 eV) | O+Sn ²⁺ (529.55 ± 0.2 eV) |
| 3.23 | 15.3 | 81.7 | 3.0 | 3.9 | 17.4 | 78.7 |
| 3.85 | 3.8 | 90.6 | 5.6 | 2.7 | 4.8 | 92.5 |
| 4.46 | 5.9 | 92.2 | 1.9 | 1.1 | 5.3 | 93.6 |
| 5.06 | 5.7 | 90.5 | 3.8 | 1.1 | 9.2 | 89.7 |

Reference

- (1) Nomura, K.; Kamiya, T.; Hosono, H. Ambipolar Oxide Thin-Film Transistor. *Adv. Mater.* **2011**, *23*, 3431–3434.
- (2) Han, Y.; Choi, Y.; Jeong, C.; Lee, D.; Song, S.-H.; Kwon, H.-I. Environment-Dependent Bias Stress Stability of *p*-Type SnO Thin-Film Transistors. *IEEE Electron Device Lett.* **2015**, *36*, 466–468.
- (3) Luo, H.; Liang, L. Y.; Liu, Q.; Cao, H. T. Magnetron-Sputtered SnO Thin Films for *p*-Type and Ambipolar TFT Applications. *ECS J. Solid State Sci. Technol.* **2014**, *3*, Q3091–Q3094.
- (4) Dhananjay; Chu, C.-W.; Ou, C.-W.; Wu, M.-C.; Ho, Z.-Y.; Ho, K.-C.; Lee, S.-W. Complementary Inverter Circuits Based on *p*-SnO₂ and *n*-In₂O₃ Thin Film Transistors. *Appl. Phys. Lett.* **2008**, *92*, 232103.
- (5) Ou, C.-W.; Dhananjay; Ho, Z. Y.; Chuang, Y.-C.; Cheng, S.-S.; Wu, M.-C.; Ho, K.-C.; Chu, C.-W. Anomalous *p*-Channel Amorphous Oxide Transistors Based on Tin Oxide and Their Complementary Circuits. *Appl. Phys. Lett.* **2008**, *92*, 122113.
- (6) Liang, L. Y.; Liu, Z. M.; Cao, H. T.; Yu, Z.; Shi, Y. Y.; Chen, A. H.; Zhang, H. Z.; Fang, Y. Q.; Sun, X. L. Phase and Optical Characterizations of Annealed SnO Thin Films and Their *p*-Type TFT Application. *J. Electrochem. Soc.* **2010**, *157*, H598–H602.
- (7) Okamura, K.; Nasr, B.; Brand, R. A.; Hahn, H. Solution-Processed Oxide Semiconductor SnO in *p*-Channel Thin-Film Transistors. *J. Mater. Chem.* **2012**, *22*, 4607–4610.